Formation of Interfacial Area at High Rates of Gas Flow Through Submerged Orifices

H. K. ABDEL-AAL, G. B. STILES, and C. D. HOLLAND

Texas A&M University, College Station, Texas

Interfacial area was formed by passing air through orifices that were submerged horizontally beneath 4.5 ft. of each of four different liquids. The flow rates of the air ranged from 0.095 to 1.34 (st. cu. ft./min.), the diameters of the orifices ranged from 0.03125 to 0.1875 in., and the I.D. of the orifice holders ranged from 1 to 2.5 in.

The areas were measured with a photocell, a recorder, and an integrator. This combination gave the time average of the interfacial area that passed a selected plane of the column.

The interfacial area produced was correlated as a function of the physical properties of the fluids, the diameter and number of orifices per plate, and the gas flow rate.

In most gas-liquid contacting equipment, the interfacial area available for mass and heat transfer is usually indeterminate. The lack of knowledge of this important variable limits the analysis of many processes.

While the formation of interfacial area in heterogeneous systems has been under investigation for many years, most of the experiments [with the exception of those of Leibson et al. (*10*), Calderbank (*4*), and Walters and Davidson (*17*)] were performed at gas flow rates which were below those commonly employed in industrial equipment.

The research described herein was undertaken because of the lack of data on the formation of interfacial area at high gas rates in gas-liquid systems. The interfacial area was formed by passing air at a high flow rate through an orifice that was submerged beneath 4.5 ft of each of four liquids. The equipment is shown in Figures 1 and 2. In the range of gas flow rates employed, a jet of gas issued from the orifice and formed large irregular bubbles which disintegrated to form smaller, more stable bubbles as the gas flowed up through the liquid. Bubble formation in this range of flow rates is referred to as the "jetting region." This region is characterized by the formation of a large bubble or jet immediately above the orifice, followed by the disintegration into smaller bubbles as gas passes up through the column.

In the investigations reported herein, the interfacial area of the small bubbles was measured at each of five or six equally spaced locations. The first measurement was made 6 in. above the top of the orifice.

Studies of bubble formation and the formation of interfacial area have been made by use of capillary tubes, porous plates, nozzles, slots, perforated plates, and orifices (*2, 4, 6, 9, 15*). Of the numerous investigations that have been made, those reported by Leibson et al. (*10*), Scott et al. (*12*), McDonough et al. (*11*), and Calderbank (*4*) are the closest related to the present investigation. Leibson et al. (*10*) made a qualitative study of the formation of bubbles at high gas flow rates. Scott et al. (*12*) and McDonough et al. (*11*) investigated the mixing of immiscible liquids by orifice mixers. Both phases were passed through the orifices and interfacial area was measured by means of a photoelectric method.

Calderbank (*3, 4*) used a light transmittance technique to measure the time average of the interfacial area produced on sieve plates and in liquids agitated in tanks. The method developed by these workers for the measurement of the interfacial area required that the interfacial area ($cm.^{-1}$) times the optical path length (cm.) be less than 25.

Walters and Davidson (*17*) studied the motion of bubbles using high gas flow rates through single orifices.

EQUIPMENT AND OPERATING PROCEDURE

The experimental apparatus shown in Figures 1 and 2 consisted of a column, the equipment necessary to supply the air and to measure the air supply rates, and the photoelectric and electronic equipment used to measure the interfacial area. A general description of the column and the air supply equipment follows. Other details pertaining to the equipment have been given by Stiles (*13*) and Abdel (*1*). Since the experimental equipment used by Stiles and Abdel was the same except for minor details, only the equipment used by Abdel is described.

Column and Air Supply Equipment

The column, constructed of stainless steel sheets (11 gauge), was 25 in. in diameter and 72 in. in height. The top of the column was vented to the atmosphere. In order to view the bubble formation and to measure it photoelectrically, four Plexiglas windows were used, one in each quadrant. The

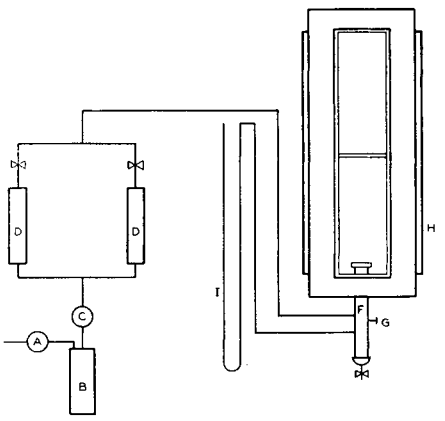

A. INLET AIR REGULATOR
B. AIR SATURATOR
C. CONTROL AIR REGULATOR
D. ROTOMETERS
E. CONTROL VALVES
F. ORIFICE HOLDER
G. DIAL THERMOMETER
H. COLUMN
I. 60 INCH MANOMETER

Fig. 1. Schematic flow diagram of equipment.

H. K. Abdel-Aal is with the National Research Council, Alexandria, United Arab Republic. G. B. Stiles is with Hdqs., APSAD, Joliet, Illinois.

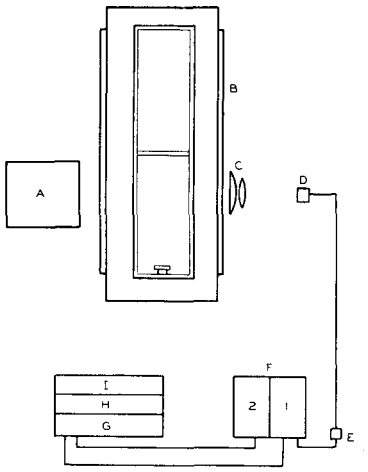

A. LIGHT SOURCE
B. COLUMN
C. CONDENSING LENS SYSTEM
D. PHOTOCELL
E. LINEARIZATION UNIT
F. TWO CHANNEL RECORDER
G. CONTROL BOX AND PATCH BOARD
H. OPERATIONAL AMPLIFIER
I. POWER SUPPLY

Fig. 2. Schematic diagram of electronic equipment.

orifice holder was inserted in the bottom of the column and extended 9 in. into the column. This orifice holder was of the same general design as that shown by Hayes et al. (*7*).

Six stainless steel orifice plates with single orifices of diameters of 0.03125, 0.0625, 0.09375, 0.1250, 0.15625, and 0.1875 in. were used. The thickness of the plates was ⅛ in. Fifteen orifice plates with multiple orifices were used. These plates were ¼-in. thick, and the orifice diameters ranged from 0.03125 to 0.125 in. and the number of orifices per plate from two to four.

The pressure of the inlet air was reduced from 90 to 35 lb./sq. in. gauge by a regulator. The air was next saturated with the vapor of the liquid under investigation by bubbling it through the liquid, which was contained in a steel pressure bomb. The pressure was further reduced from 35 to 25 lb./sq. in. gauge by use of another regulator.

The volumetric flow rate of the air was measured with two rotameters. These rotameters were calibrated with a wet test gas meter that had a capacity of 50 cu. ft./hr. The flow rate was controlled by use of ¼-in. needle values, labeled control valves in Figure 1. The pressure in the orifice holder was measured with a 60-in. manometer that used mercury as the manometer fluid. The temperatures of the air at various locations in the equipment and the temperature of the water in the column were measured with Dial thermometers.

Measurement of Interfacial Area

Systems in which the interfacial area did not vary appreciably with respect to time have been examined by numerous investigators (*9, 11, 12, 14, 16*), who used techniques of light transmittance to measure the interfacial area. However, in the experiments described herein, the interfacial area, that passed by any reference plane in the liquid, varied markedly about some mean value. To measure this area, it was necessary to record the area at any given location as a function of time. The mean area was then obtained from an integration of a plot of the instantaneous area vs. time. This was accomplished by use of a sensitive photocell, a high-speed recorder, and an integrator. A schematic diagram of the equipment employed to measure the interfacial area appears in Figure 2.

The light source was a 500-w. projector. The lamp housing contained a set of lenses for producing a parallel beam of light and an a.c. voltage regulator was used to vary the power to the lamp and thereby control the intensity of the light produced. This regulator was in series with a constant voltage transformer that served to minimize changes in voltage and consequent changes in light intensity during a set of runs.

Two lenses, a plano-convex and a double-convex, in series as shown in Figure 2, were used to reduce the beam from a width of 7 in. to a spot the size of the window of the photocell. After the light had passed through the lense system, it was directed through a conduit with an internally blackened surface. Scattered nonparallel light was thus removed from the beam before it reached the photocell.

A selenium A2M photocell filtered for the visible spectrum was used. It had an active window area of 0.046 sq. in. The photocell was linearized with a wirewound potentiometer that had a total resistance of 1,000 ohms. Signal pickup of 60 cycle a.c. was filtered by use of a 4-μfarad capacitor in parallel with the potentiometer. The signal from the photocell was fed to a high speed recorder.

The recorder had two channels. Channel 1 recorded the signal corresponding to the instantaneous area and Channel 2 recorded the integral of the signal or the integral of the area with respect to time. Each channel had an input preamplifier and each preamplifier had identical outputs. One of the outputs of each preamplifier was fed to the amplifier that controlled the pen drive for the given channel and the other output was available for any external circuit.

The signal from the photocell was fed to the preamplifier of the first channel and the output from the preamplifier of the first channel was fed to the integrator.

The basic unit of the integrator was model UPA-2 operational amplifier. External connection of a capacitor in feedback and connection of a resistor in series with the input signal makes an integrator of the operational amplifier. The output of the integrator was fed to the preamplifier of the second channel of the recorder. The integrator was provided with a switching circuit, which has been described by Stiles (*13*). The primary purpose of this circuit was to zero the integrator at the end of each integration.

Calibration of the Photoelectric Equipment

To calibrate the photocell, that is, to obtain a relationship between the interfacial area and the intensity ratio I/I_o, photographs of a column of rising bubbles were made and the interfacial area measured therefrom. For purposes of calibration, some fairly uniform bubbles were generated by use of an orifice plate which had four orifices, each of which was 0.03125 in. in diameter.

The bubbles were photographed by use of a 2¼ × 3¼ speed graphic camera. For illumination a microflash unit with a flash duration of two-millionths of a second was used. The microflash unit was equipped with a microphone so that the unit could be activated by sound. The sound of the opening of the camera shutter was used to activate the microflash.

Kodak Tri-X film, an extremely fast film, was used and was developed in Microdol-X developer. All prints were made on Kodak Medalist F-2 paper by use of Kodak developer. The area was measured manually. Four calibration curves of the interfacial area per inch of height of column as a function of

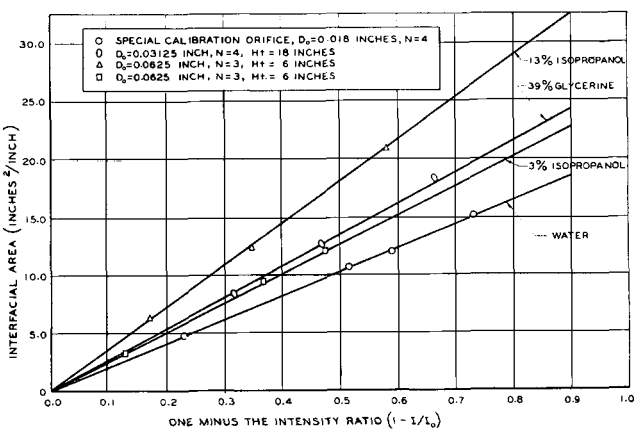

Fig. 3. Calibration curves for the photocell.

the light intensity ratio I/I_o appear in Figure 3. The equation of the curve for each liquid investigated is given by Abdel (*1*).

To obtain the relationship between the interfacial area and the intensity ratio I/I_o, several pictures were taken at each air flow rate. The average deviation of the experimental points shown in Figure 4 from the best line through them was about 2%.

Operating Procedure

Prior to making a run, the electronic equipment was allowed to warm up for 30 min. and after suitable adjustments had been made, all the operating conditions listed in Tables 3† through 9† were recorded. Several integrations of the signal from the photocell were made. There was a tendency for the stream of bubbles to move around in the column. Only the integrations made while the bubble column was centered in the window were used. To obtain reproducible values for the integrations, it was necessary that each integration be performed over a period of 5 sec.

For selected experiments, the temperatures of the gas at the outlet of the orifice and of the gas above the surface of the liquid were measured and found to be within a couple of degrees of that of the gas in the orifice holder as shown in Table 2.† The physical properties of the liquids investigated are listed in Table 1.†

The reproducibility of the experimental results for single orifices was determined by repeating forty runs. These data

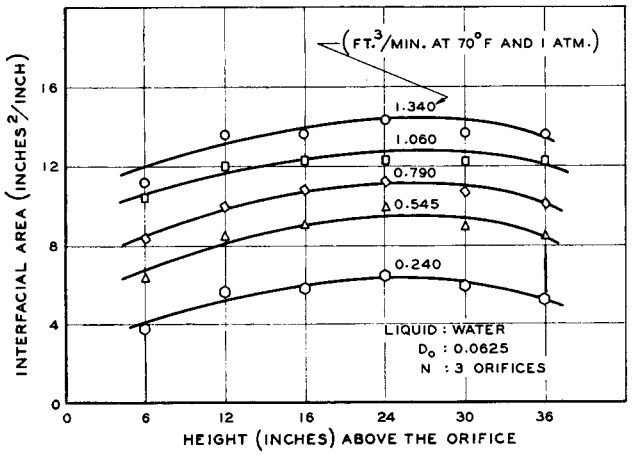

Fig. 4. Variation of interfacial area with height above the orifice.

appear in Table 9. The average deviation was 1%, the largest deviation of a repeated run was 6.6%. For multiple orifices, runs 33 to 42 of Table 6 and runs 1 to 10 of Table 7 were repeated. The average deviation was 2.0%; the largest deviation of a repeated run was 5.6%. It is estimated that there was a possible error of 2% in reading the value of the integral of the area from the chart.

INTERPRETATION OF THE EXPERIMENTAL RESULTS

The object of this work was to measure the interfacial area a which appears in the well-known expression for the rate of mass transfer:

$$r = K_G a\,(y - y^*)$$

The interfacial area a may be expressed in terms of the interfacial area produced per unit height of column. In the present work, the latter units are used and the area denoted by the symbol A.

As is evident in the photographs of reference *1*, the space immediately above the orifice holder was occupied by a

† Tabular material has been deposited as document 8650 with the American Documentation Institute, Photoduplication Service, Library of Congress, Washington 25, D. C., and may be obtained for $7.50 for photoprints or $2.75 for 35-mm. microfilm.

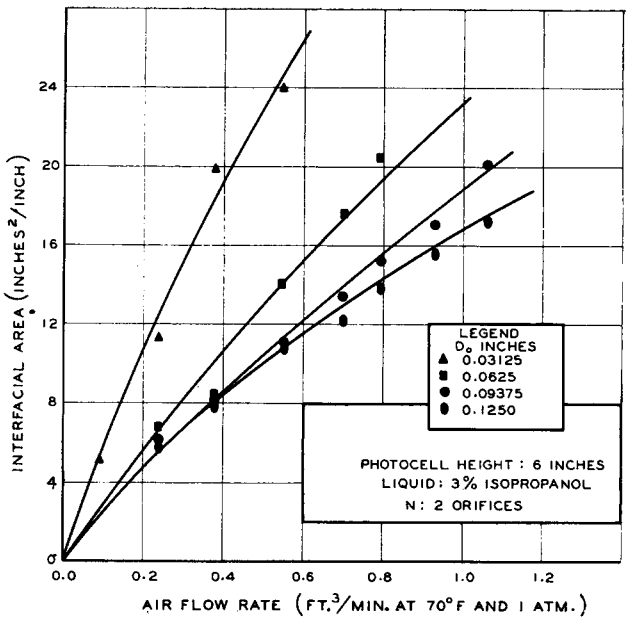

Fig. 5. Variation of interfacial area with the diameter D_o of the orifice.

large bubble or bubbles. At this location, the interfacial area was relatively small. As this large bubble of air passed up the column, it disintegrated into smaller bubbles. For the runs made with single orifices by Stiles (*13*) (see Table 9), the interfacial area increased uniformly as the bubbles passed up through the column. However, in the case of multiple orifices, the interfacial area either varied about a mean or took on a maximum value. A typical set of curves is shown in Figure 4. Also demonstrated in this figure is that the interfacial area increased as the gas rate was increased.

In Figure 5, it is demonstrated that, at a given air velocity, the smaller the orifice, the greater the interfacial area formed. As the number of orifices was increased, the interfacial area produced per orifice decreased as seen in Figure 6. As the distance between orifices was increased, the interfacial area produced per orifice increased. Although the change in the interfacial area for the small variation in the distance between orifices was small, it

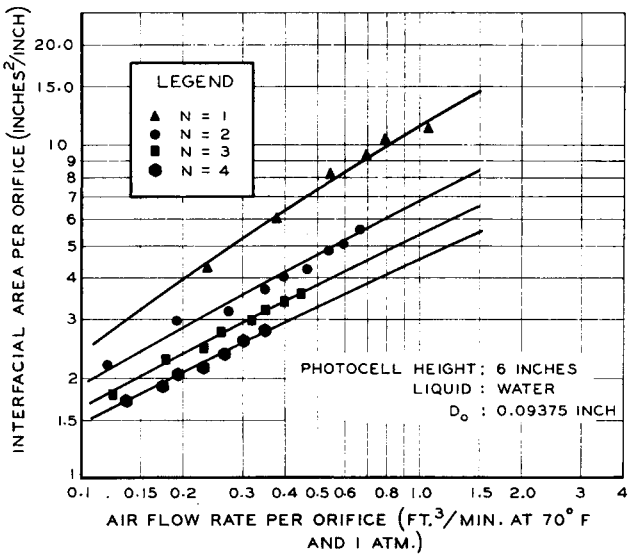

Fig. 6. Effect of the number (N) of orifices on the formation of interfacial area.

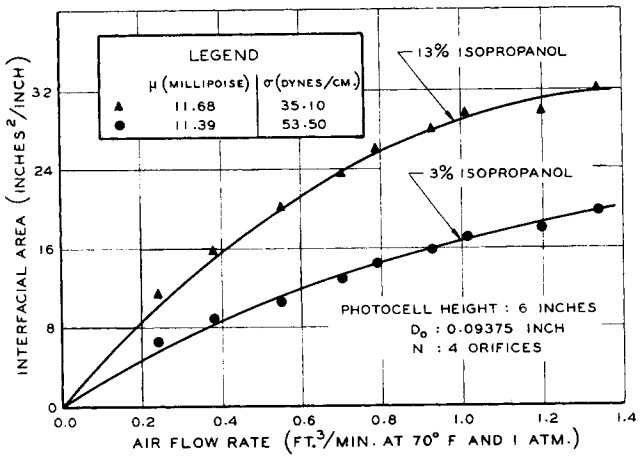

Fig. 7. Effect of surface tension on the formation of interfacial area.

was discernible. For example, for the air-water system and the case of two orifices each of diameter 0.0625 in., the interfacial area (at 6 in. above the orifice plate) increased by 7.43% when the distance between orifices was varied from 0.6 to 1.0 in. This variation of the interfacial area appeared to be almost independent of the air flow rate.

The influence of the physical properties, viscosity, and surface tension of the liquid phase on the formation of interfacial area was investigated. As the surface tension decreased, the interfacial area increased as demonstrated in Figure 7. On the other hand, as the viscosity increased, the interfacial area formed increased as shown in Figure 8.

Although the volumetric holdup of the gas in the column is not necessarily a good measure of the interfacial area, it was determined and found to vary linearly with the volumetric flow rate over the range of interest as depicted in Figure 9. The holdups were measured by means of an inclined manometer.

To investigate the effect of the diameter of the orifice holders, a series of runs was made with each of three orifice holders constructed from 1-in. steel pipe, 2-in. stainless steel pipe, and 2½-in. steel pipe. The effect of the diameter of the orifice holder on the interfacial area was almost negligible. At the lower flow rates, the interfacial area increased slightly as the diameter of the orifice holder was decreased.

In order to investigate the effect of chamber volume on bubble formation at high gas rates, two attachments (*13*) for the orifice holder were constructed. One of these attachments consisted of an insert which reduced the volume of the orifice holder from 1,380 to 120 cc., and the other attachment consisted of an extension which increased the volume of the orifice holder from 1,380 to 2,290 cc. The use of these attachments produced no change in the bubble formation from that obtained with a chamber volume of 1,380 cc. at the high gas rates used in the experiments described herein.

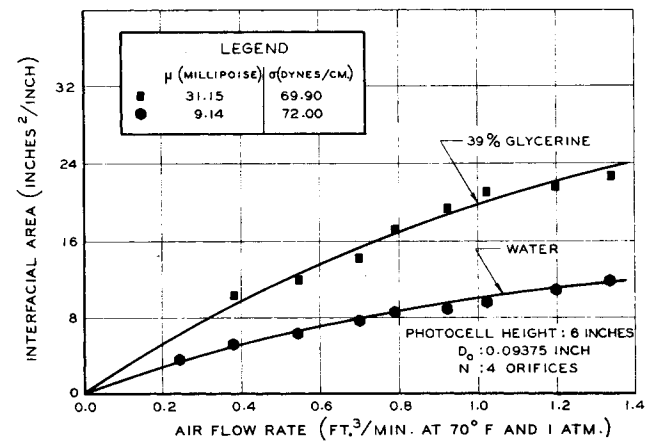

Fig. 8. Effect of the liquid viscosity on the formation of interfacial area.

CORRELATION OF THE EXPERIMENTAL RESULTS

The experimental results were analyzed on the basis of two models. The first of these, Model I, was based on energy relationships involved in the formation process. The second, Model II, was based on dimensional analysis as suggested by Hinze (*8*).

Model I

Since dimensional analysis provides little insight into the mechanism of the formation of interfacial area, the analysis that follows was undertaken. Admittedly, the final expression, Equation (12), is based on several empirical relationships; it does, however, represent the data adequately.

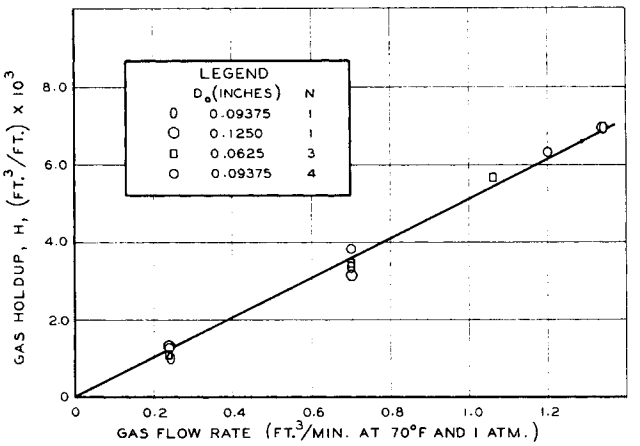

Fig. 9. Variation of the gas holdup with the volumetric flow rate.

Throughout the following analysis, the location (say 6 in. above the orifice) at which the interfacial area is examined is held fixed.

At the given location, the surface energy contained per unit height of column is given by $A\sigma$. This is also the energy required to form the interfacial area possessed by a unit height of column when the process of formation is carried out at essentially zero velocity so that viscous forces are not involved.

The energy available for the formation of interfacial area is easily deduced by making a few elementary observations. First, it is to be observed that, because of the net buoyancy force $V_g(\rho_L - \rho_g)$ that acts on a body of volume V and density ρ_g immersed in a fluid of density $\rho_L (\rho_g < \rho_L)$ and at a location just above the orifice plate, it will rise to the surface of the liquid. Regardless of the initial velocity of a bubble at the top of the orifice plate (that is, whether the velocity is zero or whether it is either equal to or less than or equal to or greater than its terminal velocity), the bubble will not only rise to the surface of the liquid, but will also tend to approach its terminal velocity as it passes up through the liquid. Thus, the kinetic energy of the gas that is in excess of that corresponding to its terminal velocity may be regarded as energy available for the formation of interfacial area and for the creation of motion in the liquid phase. Since the terminal velocity of the gas bubbles was negligible com-

pared with the velocity u_o of the gas leaving the orifice, the excess energy (ΔE) per pound mass of gas flowing is given approximately by

$$\Delta E = u_o^2/2g_c \tag{1}$$

The excess energy which does not go into surface energy must be dissipated by fluid motion; that is

$$\text{Excess energy} = \text{Surface energy} + \text{energy dissipated by fluid motion} \tag{2}$$

Since this equation requires that the energies be stated in the same units, let the surface energy be divided by the gas holdup H (cubic feet of gas holdup per foot of height of liquid) and the density ρ_g of the gas bubbles to give $(A\sigma)/(H\rho_g)$ which has the units of energy per pound mass of fluid flowing. From Figure 9, it follows that

$$H = kq \tag{3}$$

which implies that the average velocity u_t at which the gas passes up through the column is constant, since

$$H = q/u_t$$

Thus

$$\Delta E\, \rho_g\, q \propto A\sigma \tag{4}$$

In the type of bubble formation depicted in Figures 6 and 7, the flow or circulation of the liquid in the region where the interfacial area is formed is of a random nature. Deformed globules are sheared into small droplets by the turbulent, random motion of the liquid. To describe this random motion of the liquid, a characteristic length L and a mixing velocity $\bar{u}$ are needed. Three lengths, D_o, D_p, and $\sqrt{H}$, exist. Since $H = kq$, it follows that

$$\sqrt{H} \propto \sqrt{q}$$

In view of this proportionality, the $\sqrt{q}$ is referred to as a length, although it actually has the units of cubic feet per second to the one-half power in all of the correlations. The use of either D_o or $\sqrt{q}$ as characteristic lengths resulted in correlations that were about equally good; whereas, poorer correlations were obtained with D_p. For the sake of definiteness in the following analysis, let

$$L = k_o D_o \tag{5}$$

Two velocities u_o and u_p of the gas in the system were known. However, since the interfacial area formed was almost independent of D_p at a given q, it was also nearly independent of u_p at a given q. Note that $q = u_p(\pi D_p^2)/4$. Thus, it is reasonable to postulate that the mixing velocity is given by

$$\bar{u} = k_1 u_o N_D^{\,a} \tag{6}$$

where N_D is the ratio of two lengths, say D_o and $\sqrt{q}$. (Note that N_D is not dimensionless when one of the lengths is either q or $\sqrt{q}$.)

The random motion of the liquid not only dissipates energy, but at the same time creates interfacial area. The energy associated with the random motion of the liquid may be approximated in the following manner. Let τ denote the shearing force per unit of shearing area of the liquid. Now suppose that for each unit of interfacial area produced, a proportional amount of shear surface of liquid is involved, and that this liquid surface is moved past another liquid shear surface of equal area, a distance proportional to the characteristic length L. On the basis of these suppositions, the shearing energy per unit height of column is proportional to τAD_o. Since the random motion of the liquid depends upon the excess energy available, it follows that

$$\Delta E\, \rho_g\, q \propto \tau AD_o \tag{7}$$

If this expression for the shearing energy were exact, then the excess energy would be exactly equal to the sum of the surface energy $A\sigma$ and the shearing energy τAD_o. In view of the approximate form of the latter, it is appropriate to write

$$\Delta E\, \rho_g\, q = f[(A\sigma), (\tau AD_o)]$$

Now if $A\sigma$ is selected as the dependent variable, it follows that

$$A\sigma = F[(\Delta E\, \rho_g\, q), (\tau AD_o), N] \tag{8}$$

where the fact that A depends upon the number of orifices N has been included. It was found that the experimental results could be represented by taking F to be a power function of the three terms involved as follows:

$$A\sigma = K_o(\Delta E\, \rho_g\, q)^a\, (\tau AD_o)^b\, N^e \tag{9}$$

The shearing force was approximated by

$$\tau = \frac{C_D\, \rho_L\, \bar{u}^2}{2g_c} \tag{10}$$

The drag coefficient was taken to be a power function of a Reynolds number that was based on the physical properties ρ_L, μ_L of the liquid, the characteristic length L, and the mixing velocity $\bar{u}$.

$$C_D = k_2 \left(\frac{D_o\, u_o\, \rho_L}{\mu_L}\right)^{c/b} N_D^{\,cd/b} = k_2\, N_{Re}^{\,c/d}\, N_D^{\,cd/b} \tag{11}$$

When the expressions given for τ and C_D by Equations (10) and (11), respectively, are substituted in Equation (9), and the resulting expression is solved explicitly for the interfacial area, the following result is obtained.

$$A\sigma = K(\Delta E\, \rho_g\, q)^a\, N_{We}^{\,\beta}\, N_{Re}^{\,\gamma}\, N^\delta\, N_D^{\,\epsilon} \tag{12}$$

The constants and powers in Equation (12) were determined by the method of least squares for several choices of N_D, namely, D_o/D_p, $D_o/\sqrt{q}$, $D_o^2/(\sqrt{q}D_p)$, and $(D_oD_p)/q$ as shown by Adbel (*1*). The best correlation was obtained by taking $N_D = D_o/\sqrt{q}$. A digital computer was used to make the computations. Approximately equal weight was given to the data for each liquid. A total of four hundred fifty experimental observations was used. For $N_D = D_o/\sqrt{q}$, the expression

$$A\sigma = 107.10\, (\Delta E\, \rho_g\, q)^{0.634}\, N_{We}^{\,0.0837}\, N_{Re}^{\,-0.670}\, N^{1.238} \left(\frac{D_o}{\sqrt{q}}\right)^{2.724} \tag{13}$$

was obtained. The correlation coefficient was 0.973, and the average of the absolute deviations was 6.82%. The average net deviation of the areas obtained experimentally from those calculated by use of Equation (13) for liquids 1 through 4 were 0.472%, −0.142%, −2.317%, and 3.617%, respectively. A comparison of the calculated and experimental results is presented graphically in Figure 10.

Model II

When the formation of interfacial area is analyzed by dimensional analysis, and it is supposed that the area formed depends on the orifice diameter D_o, the diameter of the orifice holder, D_p, the velocity u_o, the viscosity μ_L, the density ρ_L, and the interfacial tension σ of the liquid phase, the result obtained is

$$A/D_o = K\, N_{We}^{\,\beta}\, N_{Re}^{\,\gamma}\, N_D^{\,\epsilon} \tag{14}$$

Expressions involving only the two groups N_{We} and N_{Re} for the formation of interfacial area have been proposed by Hinze (*8*). However, in the present system, where the force of gravity plays a significant role in the dissipation of energy, the local acceleration of gravity g should be in-

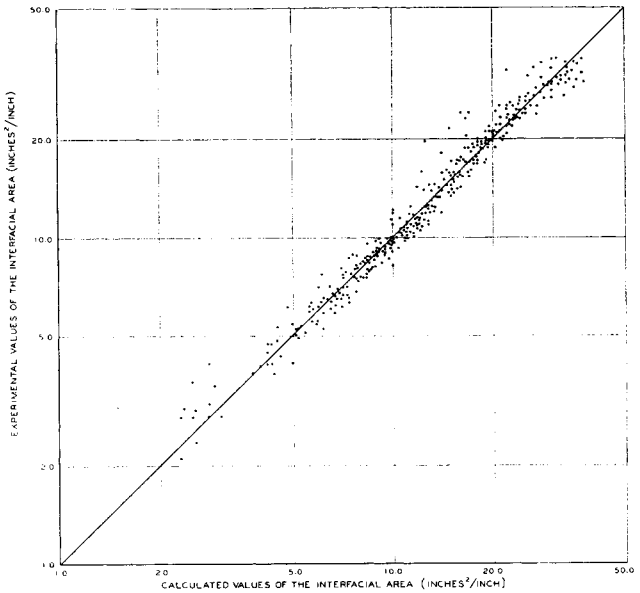

Fig. 10. Comparison of the calculated and experimental values of the interfacial area.

cluded as a variable in the dimensional analysis. When g and N, the number of orifices, are included, the result is

$$A/D_o = K N_{Fr}^{\alpha} N_{We}^{\beta} N_{Re}^{\gamma} N^{\delta} N_D^{\epsilon} \qquad (15)$$

Strictly speaking, the only independent length dimensions were D_o and D_p. Thus, $N_D = D_o/D_p$. The corresponding values of the constant and powers are given by Abdel (*1*). The correlation coefficient was 0.836 and the average of the absolute deviations of the experimental values of the areas from the corresponding ones calculated by use of Equation (15) with the appropriate constant and powers was 14.55. Certain other choices for N_D [namely, $D_o/\sqrt{q}$, $D_o^2/(\sqrt{q}D_p)$, and $(D_oD_p)/q$] were investigated (*1*). Again, as in the case of Model I, the choice $N_D = D_o/\sqrt{q}$ gave the best correlation. For this case

$$\frac{A}{D_o} = 1.897\, N_{Fr}^{0.894} N_{We}^{1.408} N_{Re}^{-0.488} N^{3.991} \left(\frac{D_o}{\sqrt{q}}\right)^{6.963} \qquad (16)$$

The correlation coefficient was 0.946, and the average of the absolute deviations was 6.86%.

CONCLUSIONS

For the liquids considered and over the jetting range of gas velocities and orifice geometrics employed, it can be concluded that the formation of interfacial area is a function of the kinetic energy at the orifice, the energy required to overcome the viscous forces in the liquid phase, and the holdup (or volumetric flow rate). In the jetting region, the interfacial area is independent of the volume of the orifice holder and almost independent of the diameter of the orifice holder.

ACKNOWLEDGMENT

This work was supported by the National Science Foundation, and by the Texas Engineering Experiment Station. This aid is gratefully acknowledged. Also, the helpful suggestions made by Professor P. T. Eubank are appreciated.

NOTATION

a = interfacial area per unit volume of column, ft.$^{-1}$; also used to denote a constant in the development of Equation (9)

A = interfacial area of the dispersed phase, air, per unit of column height measured at a given distance above the orifice, sq. ft./ft.

C_D = drag coefficient; defined by Equation (10), dimensionless

D_p = I.D. of the orifice holder, ft.

D_o = diameter of the orifice, ft.

ΔE = kinetic energy at the orifice, $u_o^2/2g_c$, (ft.)(lb.$_f$)/(lb.$_m$)

F = function defined by Equation (8)

g = local acceleration of gravity, ft./sec.^{2}

g_c = conversion factor, $g_c = 32.17$, (lb.$_m$)(ft.)/(sec.^{2})(lb.$_f$)

H = gas holdup, cu. ft./ft.

K_G = overall coefficient for mass transfer; defined by Equation (1), moles/(sq. ft.)(sec.)

k,k_0,k_1,k_2 = constants

K = constant

L = characteristic length; $L = k_oD_o$, ft.

N = number of orifices in the orifice plate

N_D = ratio of lengths. Note that for $N_D = D_o/\sqrt{q}$ (where q has the dimensions of cu. ft./sec.^{1}, N_D has the dimension of sec.$^{1/2}$/ft.$^{1/2}$

N_{Fr} = Froude number, $u_o^2/(gD_o)$

N_{Re} = Reynolds number, $D_ou_o\rho_L/\mu_L$

N_{We} = Webers number, $D_ou_o^2\rho_L/\sigma g_c$

q = volumetric flow rate, cu. ft./sec.; evaluated at a pressure equal to atmospheric plus the hydrostatic pressure corresponding to one half of the total height of liquid above the orifice and at the temperature of the liquid

r = rate of mass transfer, moles/(sec.)(cu. ft.)

u_o = linear velocity of the gas through each orifice, ft./sec.; evaluated at the pressure in the liquid at the orifice holder and at the temperature of the liquid

u_p = linear velocity of the gas in the orifice holder, ft./sec.

$\bar{u}$ = mixing velocity, related to u_o by Equation (6), ft./sec.

u_t = average velocity at which the gas passes up through the column, ft./sec.

y,y^* = mole fractions

Greek Letters

$\alpha,\beta,\gamma,\delta,\epsilon$ = constants

μ_L = viscosity of the liquid, lb.$_m$/(ft.)(sec.); evaluated at the temperature of the liquid in the column

π = 3.1416 radians

ρ_g = density of the gas, lb.$_m$/cu. ft.; evaluated at the same conditions as q

ρ_L = density of the liquid, lb.$_m$/cu. ft.; evaluated at the temperature of the liquid in the column

σ = interfacial tension of the liquid respect to air, (lb.$_f$)(ft.)/sq. ft.; evaluated at the temperature of the liquid in the column

LITERATURE CITED

1. Abdel-Aal, H. K., Dissertation, Texas A&M Univ., College Station (1965).
2. Benzing, R. J., and J. E. Myers, *Ind. Eng. Chem.*, **47**, No. 10, 2087 (1955).
3. Calderbank, P. H., *Trans. Inst. Chem. Engrs.*, **36**, 443 (1958).
4. *Ibid.*, **37**, 173 (1959).
5. Davidson, J. F., and B. O. G. Schuler, *ibid.*, **28**, 144 (1960).
6. Eversole, W. G., G. H. Wagner, and E. Stackhouse, *Ind. Eng. Chem.*, **33**, 1459 (1941).
7. Hayes, W. B., III, B. W. Hardy, and C. D. Holland, *A.I.Ch.E. J.*, **5**, No. 3, 319 (1959).
8. Hinze, J. O., *ibid.*, **1**, 289 (1955).

9. Langlois, G. E., J. E. Gullberg, and Theodore Vermeulen, *Rev. Sci. Instr.*, 25, 360 (1954).
10. Leibson, Irving, E. G. Holcombe, A. G. Cacoso, and J. J. Jacmic, *A.I.Ch.E. J.*, 2, No. 3, 300 (1956).
11. McDonough, J. A., W. J. Tomme, and C. D. Holland, *ibid.*, 6, 615 (1960).
12. Scott, L. S., W. B. Hayes III, and C. D. Holland, *ibid.*, 4, 346 (1958).
13. Stiles, G. B., Dissertation, Texas A&M Univ., College Station (1964).
14. Trice, V. G., Jr., and W. A. Rodger, *A.I.Ch.E. J.*, 2, 205 (1956).
15. Van Krevelen, D. W., and P. J. Hoftijzer, *Chem. Eng. Progr.*, 46, 29 (1950).
16. Vermeulen, Theodore, G. M. Williams, and G. E. Langlois, *ibid.*, 51, 85 (1955).
17. Walters, J. K., and J. F. Davidson, *J. Fluid Mech.*, 17, 321 (1963).

Manuscript received May 18, 1965; revision received September 23, 1965; paper accepted September 24, 1965.

A Computational Model for the Structure of Porous Materials Employed in Catalysis

RICHARD N. FOSTER and JOHN B. BUTT

Yale University, New Haven, Connecticut

A computational model for the structure of porous materials such as those employed in catalysis is proposed. The void volume within the solid is considered to be composed of two major arrays of pores, centrally convergent and centrally divergent, respectively, interconnected at specified intervals within the arrays. The exact shape of these arrays is determined uniquely from the volume-area distribution of the porous structure.

The model is applied to computation of counterdiffusional flux through a porous solid as measured in a Wicke-Kallenbach experiment. The effects of dead end pores and of mixing on the results are discussed, and comparison with experimental data reported for a particularly well-defined system is given.

The importance of internal or pore diffusion processes in catalysis has been recognized for a number of years. Various applications to problems of simultaneous diffusion and reaction have been detailed by many workers (*1*), and it has been shown that the process of mass transport within a porous solid is a highly complex one which is strongly affected by the nature of the porous structure itself. Most often these effects have been incorporated into an effective diffusivity definition which is then employed as a parameter in the solution of the normal diffusion equation; however, there are grounds for serious doubts as to whether the effective diffusivity approach alone can properly describe such mass transport processes.

Several attempts have been made to relate in quantitative fashion the effective diffusivity to properties associated with the structure of the porous matrix. Wheeler (*2*) approached the problem by assuming that the effective diffusivity of a gas in a porous material was proportional to the ordinary bulk diffusivity. The constant of proportionality was called the *labyrinth factor* or *tortuosity*. Hoogschagen (3) noted in his review of theories concerning tortuosity that various developments, particularly those of Bruggeman (*4*) and Maxwell (*5*), lead to somewhat different results. Further, actual measurements of tortuosity were not easily explained in terms of properties of the porous solid and the quantity could not be extrapolated reliably. The basic weakness of such theory resides in the fact that the effective diffusivity within a porous matrix is probably not directly proportional to the bulk diffusivity, but is a complex function of bulk diffusivity, Knudsen diffusivity, and the pore structure geometry.

A theory providing more detail results from the use of a macropore-micropore model, in which the solid is viewed as consisting of small, individual particles, each possessing a micropore structure, agglomerated into a pellet or tablet in which the macropore structure is formed by the process of manufacture. This model has been used in a considerable amount of work dealing with catalytic effectiveness and selectivity (*6, 7*), but the relationship of effective diffusivity to the individual pore structure is not defined by the model.

The point is that an overall description of the porous matrix cannot define pore structure effects; one must consider the transport process in individual pores and then assemble this into an appropriate overall description. The basis for this is provided by the analysis of Scott and